Journal of Low Temperature Physics, Vol. 139, Nos. 1/2, April 2005 (© 2005)
DOI: 10.1007/s10909-005-3911-6

Temperature and Frequency Dependence of Complex Conductance of Ultrathin $YBa_2Cu_3O_{7-x}$ Films: Observation of Vortex–Antivortex Pair Unbinding

V.A. Gasparov[*], G.E. Tsydynzhapov[*], I.E. Batov[**] and Qi Li[***]

[*] *Institute of Solid State Physics RAS, 142432, Chernogolovka, Russia*
[**] *University of Erlangen-Nürnberg, Erwin-Rommel-Str.1, D-91058, Germany*
[***] *Department of Physics, Penn. State Univ., University Park, PA 16802, USA*

We have studied the temperature dependencies of the complex sheet conductance, $\sigma(\omega, T)$, of 1–3 unit cell (UC) thick $YBa_2Cu_3O_{7-x}$ films sandwiched between semiconducting $Pr_{0.6}Y_{0.4}Ba_2Cu_3O_{7-x}$ layers at high frequencies. Experiments have been carried out in a frequency range between: 2–30 MHz with one-spiral coil technique, in 100 MHz–1 GHz frequency range with a new technique using a single spiral coil cavity, and at 30 GHz by aid of a resonant cavity technique. The real, $\mathrm{Re}\, M(T)$, and imaginary parts of the mutual-inductance $M(T, \omega)$, between a coil and a film, were measured and converted to complex conductivity by aid of the inversion procedure. We have found quadratic temperature dependence of the kinetic inductance, $L_k^{-1}(T)$, at low temperatures independent of frequency, with a break in slope at T_{BKT}^{dc}, the maximum of real part of conductance and large shift of the onset temperature and the maximum $\omega\sigma_1(T)$ position to higher temperatures with increasing frequency ω. We obtain from these data the universal ratio $T_{BKT}^{dc}/L_k^{-1}(T_{BKT}^{dc}) = 25$, 25, and 17 nHK for 1, 2 and 3-UC films, respectively in close relation with theoretical prediction of 12 nHK for vortex–antivortex unbinding transition. The activated temperature dependence of the vortex diffusion constant was observed and discussed in the framework of vortex–antivortex pair pinning.

PACS numbers: 74.80.Dm, 74.25.Nf, 74.72.Bk, 74.76.Bz.

1. INTRODUCTION

Although, many observations of the Berezinski–Kosterlitz–Thouless (BKT) transition in YBCO,[1–12] BiSrCaCuO,[13,14] and TlBaCaCuO[15] com-

pounds have been reported, detailed comparison of the experimental data with the theory by Davis *et al.*[16] showed disagreements possibly due to inhomogeneity and vortex pinning. Rogers *et al.* reported that the usual BKT transition, i.e. all thermally activated vortices form vortex–antivortex pairs at temperatures below BKT transition temperature T_{BKT}, was not observed in ultrathin $Bi_2Sr_2Cu_2O_8$ films from a low-frequency noise measurement due to vortex pinning.[17] Repaci *et al.*[18] showed from the study of *dc* I–V curves that free vortices exist even at low temperatures even in one unit cell (UC) thick YBCO films, indicating the absence of the BKT transition. The binding energy between a vortex-antivortex pair $U(r) \propto 1/r$ diverges at high distances $r > \lambda_{eff}$ (here $\lambda_{eff} = 2\lambda^2/d$ is the effective penetration depth and d is the film thickness).[19] Thus they have pointed out that a precondition[19] for the BKT transition to occur in a superconductor, i.e. the sample size $L_s < \lambda_{eff}$, is not satisfied in YBCO films as thin as one unit cell.

According to the BKT theory extended to finite frequencies,[20–22] higher frequency currents sense vortex–antivortex pairs of smaller separations. A high frequency, the electromagnetic response of a 2D superconductor is dominated by those bound pairs that have $r \sim l_\omega$, where $l_\omega = (14D/\omega)^{1/}$ is the vortex diffusion length and D is the vortex diffusion constant. Using the Bardeen-Stephen formula for free vortices, $D = 2e^2\xi_{GL}^2 k_B T/\pi\hbar^2\sigma_n$ (Ref. 23), we estimate that $l_\omega < 1$ μm at $\omega \geq 10$ MHz, which is muc less than $\lambda_{eff} \sim 40$ μm for the 1-UC YBCO film. This implies that it is possible to detect the response of vortex–antivortex pairs with short separation lengths at high frequencies in the samples even though the usual BKT transition is not present as shown in *dc* and low frequency measurements.

In this paper, we report the frequency and temperature dependencies of the complex sheet conductance, $\sigma(\omega, T)$, of 1-UC to 3-UC thick YBCO films sandwiched between semiconducting $Pr_{0.6}Y_{0.4}Ba_2Cu_3O_{7-\delta}$ layers in frequency range between 1 MHz to 30 GHz. Here $\sigma(\omega, T) = \sigma_1(\omega, T) - i[\omega L_k(\omega, T)]^{-1}$, where $\sigma_1(\omega, T)$ is the dissipative component of the sheet conductance and $L_k(\omega, T) = \mu_0\lambda^2/d$ is the sheet kinetic inductance (μ_0 the permeability of free space). In the frequency range of our measurements, the condition $l_\omega \sim r < \lambda_{eff}$ is met. Preliminary results of this study hav been published in Ref. 24.

We found a large increase of $T_{BKT}(\omega)$ as a function of frequency for those films from 4 MHz to 30 GHz. A jump of $L_k^{-1}(T)$, a maximum of $\sigma_1(T$ at T_{BKT}^{ω}, and the scaling of the universal superfluid jump close to the theoretical prediction at the frequencies studied was observed. The superfluid jump is suppressed in a very small magnetic field. Vortex pinning with thermally activated vortex diffusion constant was found in the samples, while it did not destroy the vortex–antivortex pairs with short separation lengths.

2. EXPERIMENTAL SETUP

Ultrathin YBCO layers sandwiched between 100 Å buffer and 50 Å cover layers of $Pr_{0.6}Y_{0.4}Ba_2Cu_3O_{7-d}$ were grown epitaxially on atomically flat and well-lattice-matched (100) $LaAlO_3$ substrates using a multitarget pulsed-laser deposition (PLD) system with computer-controlled laser triggering. The microstructure, growth mechanism of similar atomically flat films made by PLD, and their various superconducting properties have been studied before.[2,18,25–27] For few UC thick films and the substrate used, the thicknesses are below the critical value for forming islands and the growth is in the range of layer by layer Stranski-Krastanov growth. The sample thickness is rather uniform due to the nature of the growth mode as characterized by using cross sectional transmission electron microscopy (TEM), atomic force microscope (AFM) and in situ RHEED. The three films thickness we examined were nominally 1, 2, and 3 unit cells thick and had the c axis normal to the film surface. The samples were made at different oxygen composition and therefore we will call them as S1 and S2 ones. The contacts were made at the edges of the $1 \times 1 cm^2$ 3UC film for van der Pauw four-point resistance measurements.

The $\sigma(\omega, T)$ at RF in thin films was investigated employing a single coil mutual inductance technique. This technique, originally proposed in Ref. 28 and lately improved in Ref. 29, has the advantages of the well known two-coil geometry,[30,31] and was extensively used for the study of the $\lambda(T)$ dependence for YBCO and MgB_2 films.[9,28,32,33] In this radio frequency technique, the change of inductance ΔL of a one-layer pancake coil located in the proximity of the film and connected in parallel with a capacitor C is measured. The LC circuit is driven by the impedance meter (VM-508 TESLA) operating at 2–50 MHz, with a high frequency stability of 10 Hz. The film is placed at small distance (~ 0.1 mm) below the coil and is thermally insulated from the coil by Teflon foil. Both sample and coil are in a vacuum, but the coil holder is thermally connected with helium bath, while the sample holder is isolated and may be heated. During the experiment the coil was kept at 4.2 K, whereas the sample temperature was varied from 10 K to 100 K. Such design allows us to eliminate possible effects in temperature changes in L and C on the measurements.

The complex mutual inductance M between the coil and the film can be obtained through:

$$\mathrm{Re}\, M(T) = L_0 \cdot \left(\frac{f_0^2}{f^2(T)} - 1 \right), \tag{1}$$

$$\mathrm{Im}\, M(T) = \frac{1}{(2\pi f(T))^3 C^2} \cdot \left[\frac{1}{Z(T)} - \frac{1}{Z_0(T)} \cdot \frac{f^2(T)}{f_0^2} \right]. \tag{2}$$

Here L, $Z(T)$, $f(T)$, L_0, Z_0 and f_0 are the inductance, impedance and the resonant frequency of the circuit with and without the sample, respectively. In the low frequency regime, where the coil wire diameter is much thinner than the skin depth at the working frequency, the expression of the variation of the $M(T)$ (relative to the case where no sample is in the coil, M_0) as a function of the $\sigma(T)$ may written as:

$$\Delta M(T) = \pi\mu_0 \cdot \int_0^\infty \frac{M(q)}{1 + 2ql\coth(d/l)}\, dq, \tag{3}$$

where μ_0 is the permeability of vacuum, $M(q)$ plays the role of mutual inductance at a given wave number q in the film plane and depends on the sample-coil distance h, d is the sample thickness, and l is a complex length defined as $l = [1/(i\omega\mu_0\sigma_1 + \lambda^{-2})]^{1/2}$, (more details can be found in Ref. 29). A change in real, $\mathrm{Re}\, M(T)$, and imaginary, $\mathrm{Im}\, M(T)$, parts of $M(T)$ were detected as a change of resonant frequency $f(T)$ of the oscillating signal and impedance $Z(T)$ of the LC circuit, and converted into $L_k^{-1}(T)$ and $\sigma_1(T)$ by both using (1), (2) and (3) and inversion mathematical procedure.

The high frequency (HF) measurements (100 MHz - 1 GHz) were performed using the cavity formed with a similar spiral coil with no capacity in parallel. The coil form the radio frequency resonator coupled to a two coupling loops and is driven by the radio-frequency signal generator/receiver (from 100 MHz to 1 GHz). In this case the quality factor of the resonator Q and the resonance frequency were measured and converted to $\mathrm{Re}\, M(T)$ by (1) and to $\mathrm{Im}\, M(T)$ by:

$$\mathrm{Im}\, M(T) = L_0 \cdot \frac{f_0^2}{f^2(T)} \cdot \left[\frac{1}{Q(T)}\frac{f_0^2}{f^2(T)} - \frac{1}{Q_0}\right], \tag{4}$$

where $Q(T)$ and $Q_0(T)$ are the quality factors with and without the samples, respectively.

The MW losses were measured using a resonant cavity technique with the gold-plated copper cylindrical cavity operated in the TE_{011} mode at 29.9 GHz. The samples were mounted as a part of the bottom of the cavity through a thin gold-plated Cu-diaphragm with a small central hole, so that the sample itself occupies only the holes part of the endplate through a transparent (20μ - thick) Teflon film. The diameter of the central hole of the diaphragm varied in the experiments from 2.4 mm to 3.8 mm (the sample width was 10 mm).

The resonator was operating in a transmission configuration. Measurements were done using an experimental technique based on the amplitude technique.[24] During the experimental run, we measured the amplitude of the transmitted signal at resonance as a function of temperature. The resonator

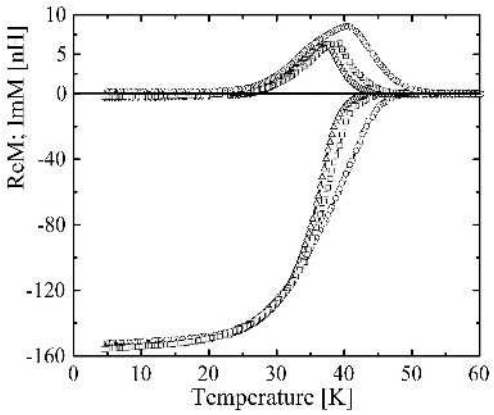

Fig. 1. The $\mathrm{Re}\, M(T)$ and $\mathrm{Im}\, M(T)$ curves for a 2-UC film (S2) at different frequencies: 3 MHz (triangles), 26 MHz (squares) and 500 MHz (circles) calculated from raw $f(T)$, $Z(T)$ and $Q(T)$ data. The solid lines describe a guide for the eye.

was coupled weakly to the input and output waveguides so the amplitude of the transmitted signal at resonance is proportional to the square of unloaded quality Q. A calibration of the transmitted signals at resonance in terms of the absolute value of Q was made by measuring the bandwidth of the cavity at fixed temperature. We assume the MW electric field E in the film to be uniform along normal direction and equal to the E without the film. The $\sigma_1(\omega, T)$ is thus proportional to $\Delta Q^{-1}(T) = Q^{-1}(T) - Q_0^{-1}(T)$,[24] where $Q(T)$ and $Q_0(T)$ are the quality factors with and without the samples, respectively.

3. RESULTS

Figure 1 displays the $\mathrm{Re}\, M(T)$ and $\mathrm{Im}\, M(T)$ curves for a 2-UC S2 film at three different frequencies from 4 MHz to 500 MHz as measured by different techniques: LC circuit and single coil resonator. The MW data are normalized to RF $\mathrm{Re}\, M(0)$ data because of different sample-coil gap values used. $\mathrm{Re}\, M(T)/\mathrm{Re}\, M(0)$ and $\mathrm{Im}\, M(T)$ for 3-UC S2 film measured at the same frequencies are shown in Fig. 2 as a function of temperature. The most noticeable feature of the data is rather high shift of the onset point T_c of transition $\mathrm{Re}\, M$ with frequency, not observed in such measurements on thick films. Notice also, that the inductive response, $\mathrm{Re}\, M(T)$, starts at lower temperatures than $\mathrm{Im}\, M(T)$, characterized by a peak close to transition, and this shift is raised with frequency. We have carried out the mu-

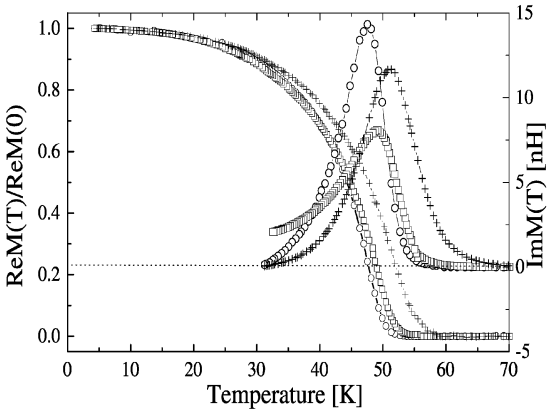

Fig. 2. The $\mathrm{Re}\, M(T)/\mathrm{Re}\, M(0)$ and $\mathrm{Im}\, M(T)$ curves for a 3-UC film (S2) at different frequencies: 3 MHz (triangles), 25 MHz (squares) and 500 MHz (circles) calculated from raw $f(T)$, $Z(T)$ and $Q(T)$ data. The solid lines describe a guide for the eye.

tual inductance measurements on $Pr_{0.6}Y_{0.4}Ba_2Cu_3O_{7-d}$ films and observed no any features in the temperature dependences of the mutual inductance $M(T)$.

The $\mathrm{Re}\, M(T)$ and $\mathrm{Im}\, M(T)$ data are converted to $L_k^{-1}(T)$ and $\mathrm{Re}\, \sigma(T)$ using Eq. 3 and the mathematical inversion procedure[24] based on the same approach as in the two-coil mutual inductance method. Fig. 3 shows the $L_k^{-1}(T)$ curves in very low perpendicular magnetic fields, and zero field $\omega \mathrm{Re}\, \sigma(T)$ for the 1-UC and 2-UC films (S1). We found that $L_k^{-1}(T)$ fit well over a wide temperature range by a parabolic dependence:[34] $L_k^{-1}(T) = L_k^{-1}(0)[1-(T/T_{c0})^2]$, shown as thin solid lines in Fig. 3. We emphasize that this quadratics equation fit the data below characteristic temperature which we define as T_{KTB}^{ω}, and which coincide with the positions of the peaks in $\omega \mathrm{Re}\, \sigma(T)$. The mean field transition temperature, T_{co}, determined by extrapolation of $L_k^{-1}(T)$ to 0, is larger than the onset of transitions of $L_k^{-1}(T)$, while is close to the onset point of $\omega \mathrm{Re}\, \sigma(T)$ curves. Also, the $L_k^{-1}(0)$ fitted data are the same for $H = 0$ and 5 mT while have different T_{c0}.

In Fig. 4, we plot $\omega \mathrm{Re}\, \sigma(T)$ at 8 MHz, $\Delta Q^{-1}(T)/Q_0^{-1}(4.2\ \mathrm{K})$ determined from MW data (30 GHz) for 3-UC sample (S1). The *dc* resistive transition of the same sample is also shown in the figure. According to the Coulomb gas scaling model, the resistance ratio R/R_n is proportional to the number of free vortices and should follow a universal function of an effective temperature scaling variable $X = T(T_{c0} - T_{BKT}^{dc})/T_{BKT}^{dc}(T_{c0} - T)$ (Ref. 20), which can be approximated by $R/R_n = C_0 X \exp[-C_1(X-1)^{-1/2}]$ (here R_n is the normal

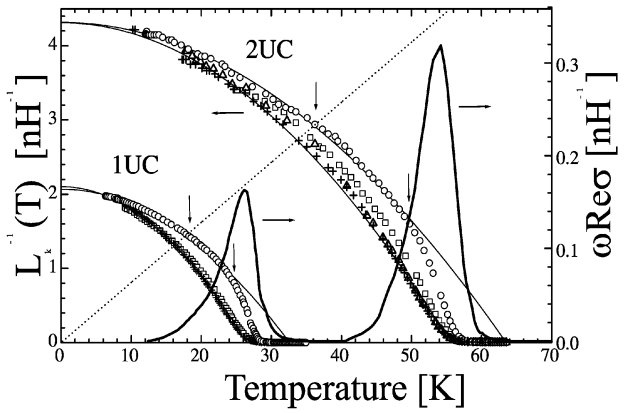

Fig. 3. Temperature dependence of $L_k^{-1}(T)$ for 1- and 2-UC films (S1) at 8 MHz and different magnetic fields: 0 (circles), 2 mT (squares), 3 mT (triangles) and 4 mT (crosses). The solid lines curves shows the real part of the conductivity near the transition temperature, $\omega Re\sigma(T)$, at zero field. The thin solid lines are quadratic fits to $L_k^{-1}(T)$ below T_{BKT}^{dc} and for magnetic field data. Also shown is the theoretical BKT function (dashed line).

state resistance, $C_0 = 1.7$ and $C_1 = 4.9$ are constants). We plot $T/X(T)$ as a function of T obtained by fitting R/R_n data for the 3-UC film with this equation in the insert of Fig. 4. The best fit was found with $T_{c0} = 78.5$ K (the point where $T/X = 0$) and $T_{BKT}^{dc} = 56$ K. Here T_{BKT}^{dc} represents a nominal *dc* BKT transition temperature which is lower then T_{BKT}^{ω} determined from RF and MW data.

There are three major features observed in our RF and MW measurements: (i) the large frequency dependence of $T_c(\omega)$, (ii) a foot jump in temperature dependence of the $L_k^{-1}(T)$, which is destroyed in weak magnetic fields, and (iii) a maximum in $\omega \mathrm{Re}\,\sigma(T)$ with the onset of transition at higher temperatures than that of the $L_k^{-1}(T)$.

Indeed, as we can see from Fig. 1, the T_{BKT}^{ω} value, determined as the maximum position of losses, increases on 4 K (from 36.6 K to 40.7 K) as the frequency raises from 3 to 500 MHz for 2-UC YBCO S2 film. The T_{BKT}^{ω} value shift at 30 GHz is much larger: 74 K as compared with 61.5 K at 8 MHz (see Fig. 4). Even larger shift of T_{BKT}^{ω} was observed in 1-UC film and no shift was detected in a 2000 Å thick YBCO film. Although dissipation peaks have been observed in other systems when the skin depth is in the order of the sample size, the estimated skin depth of our samples is several orders of magnitude smaller than the sample size, indicating that the observed loss peak is not due to the skin effect.[34]

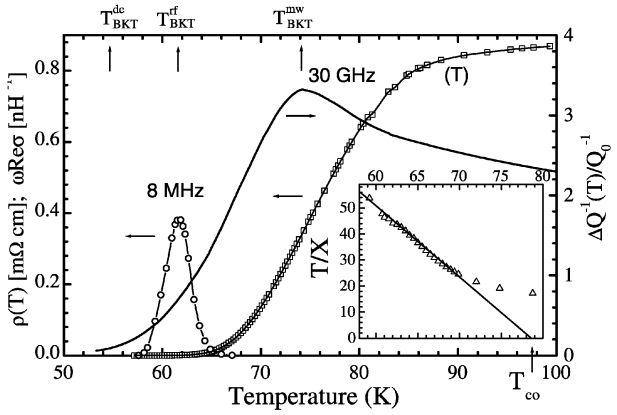

Fig. 4. Temperature dependence of *dc* $\rho(T)$, $\omega \mathrm{Re}\,\sigma(T)$ at 8 MHz and $\Delta Q^{-1}(T)/Q_o^{-1}(4.2\ K)$ at 30 GHz for a 3-UC sample (S1). Inset shows the universal plot: T/X vs T. Arrows indicate the T_{BKT} values determined from the *dc* resistivity, loss function at 8 MHz and MW measurements (30 GHz).

4. DISCUSSION

The qualitative explanation of the frequency dependence of $T_{BKT}(\omega)$ and a peak in $\sigma_1(T)$ is as following. By probing the system at finite frequencies, the observed bound-pair response is dominated by those pairs with $r \sim l_\omega$. At temperatures below T^{dc}_{BKT}, the dissipation is proportional to the number of such vortex–antivortex pairs.[20] This number grows gradually with temperature up to T^{ω}_{BKT}. At the higher temperature side, σ_1 decreases with increasing temperature since $\sigma_1 \sim 1/(n_f \mu)$, where n_f is the density of free vortices and μ is the vortex mobility.[20] Dissipation is largest when the correlation length $\xi_+(T)$, i.e. the average distance between thermally induced free vortices above T^{dc}_{BKT}, becomes equal to $l_\omega(T)$ which determines the BKT transition temperature at a given frequency T^{ω}_{BKT}.

In order to see whether this assumption is correct, we plot theoretical BKT function $L_k^{-1}(T)$ as dashed straight line on Fig. 3 derived from the universal relationship

$$L_k^{-1}(T_{BKT}) = \frac{32\pi^2 k_B T_{BKT}}{\phi_0^2 \mu_0}, \tag{5}$$

predicted by theory.[4,16] Notice however, that this theoretical dependence is valid for *dc* case, while the frequency dependence of T^{ω}_{BKT} is obvious from the picture discussed above. This is why the critical temperatures determined from the intercept of dashed theoretical line with experimental $L_k^{-1}(T)$ is

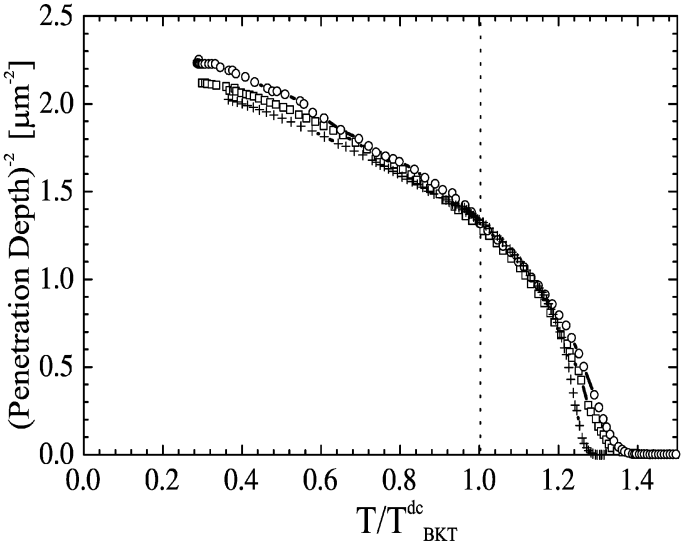

Fig. 5. The penetration depth $\lambda^{-2}(T)$ derived from $L_k(T) = \mu_0\lambda^2/d$ vs normalized temperature T/T^{ω}_{BKT} at 8 MHz for: 1UC (circles), 2UC (squares) and 3UC (crosses) S1 films.

lower then the peak of $\sigma_1(T)$ position. To see whether this description is correct, we plot the dependence of the penetration depth $\lambda^{-2}(T)$ derived from $L_k(T) = \mu_0\lambda^2/d$, versus scaling variable – normalized temperature T/T^{ω}_{BKT} on Fig. 5. It is obvious, that all data for three studied S1 films at 8 MHz fall on the same curve, which proof of our definition of T^{ω}_{BKT} as the peak position of $\sigma_1(T)$.

A central quantity in the dynamic description of BKT transition is the frequency – dependent complex dielectric function $\varepsilon(\omega)$ which describes the response of a 2D superconductor to an external time-dependent field. The measured $L_k(T)$ is renormalized from the BCS $L_{k0}(T)$ which is the $L_k(T)$ in the absence of the vortices: $L_{k0}(T)/L_k(T) = n_s/n_s^0 = \mathrm{Re}\,[1/\varepsilon(\omega)]$. It is easy to show from Ref. 20,22 the following relation in high frequency limit:

$$\frac{L_k^{-1}(T)}{\omega \mathrm{Re}\sigma} = \frac{\pi(Y-1)}{2YlnY}, \tag{6}$$

where $Y = (l_\omega/\xi_+)^2$. Both real and imaginary part of the $1/\varepsilon(\omega)$ are directly related to Y.[20] By solving Eq. 6 for $Y(T)$ using $L_k^{-1}(T)$ and $\mathrm{Re}\,\sigma(T)$ data, we obtained $Y(T)$ for different S1 samples and plotted as Y versus T^{ω}_{BKT} in Fig. 6.

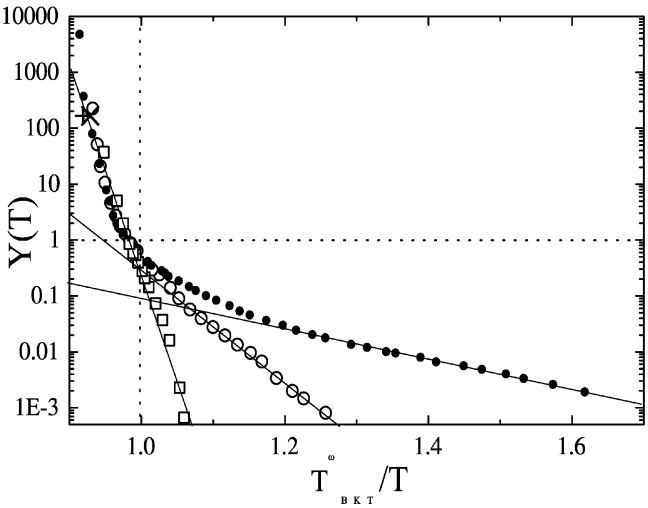

Fig. 6. The $Y(T)$ versus T^{ω}_{BKT}/T for 1- (closed circles), 2- (open circles) and 3-UC (open squares) S1 samples at 8 MHz. Crosses shows the 500 MHz data for 2- and 3-UC S2 films, respectively.

From the $Y(T)$ data, we thus found that the vortex diffusion constant $D(T)$ is not linear with T at low temperature range as in the case for free vortices,[20] but rather can be fitted with $D(T) = D_0 \exp[E_0/k_B(T_{c0}^{-1} - T^{-1})]$ due to pinning of vortex core.[23] The pinning energy, $E_0/k_B = 48\ K$, 1270 K and 3290 K for the 1, 2 and 3-UC S1 samples, can then be obtained. Notice we found stronger thickness dependence of the pinning energy than $E_0/k_B\,[\mathrm{K}] = 260d\,[\mathrm{nm}]$ in the BSCCO trilayers[17] and $E_0/k_B\,[\mathrm{K}] = 450d\,[\mathrm{nm}]$ in the YBCO/PrBCO superlattices,[39] probably due to different $\lambda(0)$ values of different samples as observed from the infrared measurements.[39]

We determined the T^{ω}_{BKT} as the peak position of $\sigma_1(T)$ point, which almost coincides with the point where $Y = 1$. We also used the T^{dc}_{BKT} as the point where $L_k^{-1}(T)$ deviates from the square fit (see Fig. 3), as was used by Hebard *et al.*[40] The ratio $T^{dc}_{BKT}/L_k^{-1}(T^{dc}_{BKT})$ then equal to 25, 25, and 17 nH K for 1-, 2- and 3-UC S1 films, respectively, is about constant, which however is larger than the theoretical estimation $T^{dc}_{BKT}\lambda^2(T^{dc}_{BKT})/d = \phi_0^2/32\pi^2 k_B = 0.98$ cm K (or $T^{dc}_{BKT}/L_k^{-1}(T^{dc}_{BKT}) = 12.3$ nH K)[22] (ignoring small dynamic theory corrections of Ambegaokar *et al.*[21] to the renormalized coupling constant K_R). When $T > T^{dc}_{BKT}$, the $Y(T^{\omega}_{BKT}/T)$ deviates from exponential lines due to temperature dependence of $\xi_+(T)$ but collapse into one curve, indicating that the temperature dependence of $\xi_+(T^{\omega}_{BKT}/T)$ is

the same for all the samples. The 500 MHz data for T_{BKT}^{ω} for 2-UC and 3-UC S2 samples were converted to RF by multiplying $Y = 1$ on the MW/RF frequency ratio since $Y \sim 1/\omega$. Notice very good agreement of these data with 8 MHz ones for S1 samples (see crosses in Fig. 6).

The Abrikosov vortex lattice parameter a_v is the scale limiting the formation of vortex–antivortex pairs in magnetic field.[41] We can estimate the field H_{ext} which destroys the vortex pair unbinding from the following relation: $l_\omega \sim a_v = (\phi_0/H_{ext})^{1/2}$. This estimation gives $H_{ext} \approx 1.5$ mT at 10 MHz for 1-UC and 2-UC films which is in good agreement with the experimental results (see Fig. 3). Since $H_{ext} \sim \omega$, we expect that a larger field is required at higher frequencies in order to destroy the unbinding transition. In fact, the magnetic field which destroys the transition at RF, did not influence the transition at MW.[24] The effect was observed at higher field (about 5 mT) at MW, but apparently it is not due to the vortex–antivortex pair unbinding but rather the normal vortex formation in a magnetic field.

Rogers *et al.* argued that the vortex–pin interaction suppresses free vortex motion rather than vortex–antivortex interaction[17] for single unit cell BiSrCaCuO 2:2:1:2. However, the measurement were done at low frequencies where the pairs detected would have $r > \lambda_{eff}$. On the other hand, vortex pinning is also present in our samples because of the exponential dependence of $D(T)$ observed. Nevertheless, the consistent picture of the frequency dependence of the data and the scaling behavior of the universal superfluid jump (Fig. 5) let us believe that vortex–antivortex interaction was indeed observed with the presence of pinning. Fisher pointed out recently that weak pinning by point defects does not affect the BKT transition,[41] but it is not clear for the case of strong pinning.

Now we turn to the discussion whether the observed frequency dependence of the σ_1 peak is due to the skin effect and the films quality rather than BKT transition. In normal metals, a dissipative peak occurs when the skin depth, $\delta = (2\rho/\mu_0\omega)^{1/2}$, is the order of the sample size. In bulk high-T_c superconductors, a frequency dependent peak in the imaginary part of the AC susceptibility $\mathrm{Im}\chi(T)$ has been indeed observed when magnetic vortices are present.[35] This is attributed to the fact that the characteristic AC penetration depth λ_{ac} is modified from the London penetration depth λ_L due to response of vortices and the $\mathrm{Im}\chi(T)$ peak occurs when λ_{ac} is about the sample size.[43]

However, in the MW measurements, the undisturbed microwave magnetic field is parallel to the film surface. The relevant sample size for parallel microwave fields is the film thickness, which is between 11.7 Å to 35.1 Å and far too small compared to the skin depth at the frequency range. Even if the disturbed microwave field may have a weak perpendicular component, we

have measured the microwave losses for different exposed sample size from 2.4 mm to 3.8 mm and observed no change in the peak position although the MW losses increased with increasing sample size. Also, if we estimate the skin depth δ by use of $\rho = 0.34 m\Omega cm$ (at maximum MW losses temperature) than we will obtain $\delta = 5.36\mu$, which is three order of magnitude less than the width of our 3UC film size (1 cm). This indicates the sample size is not related to the MW loss peak.

In the RF experiments, the external AC magnetic field generated by the coil is localized at the center of the sample. The size of the coil is much less than the sample size. The external AC field calculated at the sample edges is less than 0.5×10^{-3} G which is 0.5% of the center value and there is no external AC field penetration from the edge of the sample. This is completely different from the measurements in bulk superconductors, in which uniform AC field penetrates into the sample from the sample edge. The theories related with this effect[36,44] all deal with such configuration and therefore do not apply directly to our experiments. The analysis of our measurements is based on a well established theoretical procedure, which deals with the situation where the AC magnetic field is localized at the center of a large enough film. It was first used by Fiory et al.[45] and later by several other groups, and was further confirmed by a more complete electrodynamic theory developed by Clem and Coffey.[46,47]

Besides, we have obtained $\delta = 0.13\mu$ for the peak temperature 61.6 K at 8 MHz ($\rho = 5.36 \times 10^{-4}$ Ωcm) for the 3UC sample in Fig.4, far too small compared to a film or a coil size. To see whether the applied field propagated from a close vicinity of the coil may affect the results, we have measured the RF losses for different exposed sample size from 1 mm to 2 mm (varying a coil size) and observed no change in the Im $M(T)$ peak position.

Another problem may arise from the film structure. If there would be an island or a domain structure, the external field would penetrate the sample from weak links at the superconducting domains borders rather then from film edges. However, as was observed before by TEM and AFM techniques,[2,18,25,26] the main feature of the microstructures of our films is the atomic steps with no islands, because the thicknesses are below the critical value for forming islands. Typically, the size of a growth terrace is about few thousands $\mathring{A}$ and there are atomic steps with the height of 1-UC between terraces. Although these atomic steps may affect the superconducting properties due to the weak-links, it was shown before[2] that in the samples used in this paper, the critical current measurement $J_c(H,T)$ revealed the scaling to be similar to thick films. Notice, that our films are completely different from a thick $YBa_2Cu_3O_{7-x}$ ones where films form through two dimensional nucleation and island growth.[48]

Even if we assume that we have some kind of weak-link behaviors due to the atomic steps, the microscopic defects will not give rise to the frequency dependence of $\sigma(T)$ which is the main result of our paper. The atomic steps may affect the absolute value of the microwave surface resistance at low temperatures. However, we have only used the relative change of the surface resistance with temperature. These results suggest the absence of significant weak-link effects in these films. The increase of maximum position of $\mathrm{Re}\,\sigma(T)$ as a function of frequency observed must be from intrinsic properties of a 2-D superconductor.

In YBCO films with weak-link behaviors, Leemann *et al.*[49] have studied the mutual inductance at low frequencies and calculated the complex conductance. The scaling of the superfluid jump is larger by several factors than the prediction of the BKT theory. This has been used to judge that their samples are granular-type. Similar result was also observed by Rogers *et al.*[17] on BSCCO ultrathin films. It is generally believed that the inhomogeneity can destroy the interaction of vortex-antivortex pairs. However, inhomogeneity can never help to create the BKT transition. It is easy to see from above, we report several results which are in qualitative agreement to the prediction of the dynamic theory of vortex–antivortex pairs with short separation lengths. These effects must be from intrinsic effect and can not be the result of inhomogeneity in the samples.

5. CONCLUSIONS

In summary, we have compared our experimental results on ultrathin YBCO films with the extended dynamic theory for BKT transition and found that the vortex–antivortex pairs with short separation lengths are present. The unbinding of the vortex pairs were observable at high frequencies even though a true BKT transition is absent in the samples. Our results also indicate that part of the transition broadening in ultrathin YBCO films can be related to the dissociation of vortex–antivortex pairs.

ACKNOWLEDGEMENTS

We are grateful to V.F. Gantmakher, A. Hebard, M. Chan, R. Huguenin, C. Lobb, P. Martinoli, D. van der Marel, D. Pavuna, C. Rogers, D.J. Scalapino, J.-M. Triscone, T. Venkatesan, X.X. Xi for stimulating discussions. This work was partially supported by Russian Scientific Programs: Superconductivity of Mesoscopic and Highly Correlated Systems (Volna 4G); Surface Atomic Structures (No.4.10.99) and Russian Ministry of Industry, Sci-

ence and Technology (MSh-2169.2003.2), RFBR (No.02-02-16874-a), NSF DMR#0405502, CRDF (Award 3107) and by INTAS (No.01-0617).

REFERENCES

1. T. Terashima, K. Shimura, Y. Bando *et al.*, *Phys. Rev. Lett.* **67**, 1362 (1991).
2. C. Kwon, Qi Li, X.X. Xi *et al.*, *Appl. Phys. Lett.* **62**,1289 (1993).
3. M.Z. Cieplak S. Guha, S. Vadlamannati *et al.*, *Phys. Rev. B* **50**,12876 (1994).
4. J.M. Kosterlitz and D.J. Thouless, *J. Phys. C* **6**, 1181 (1973); *Prog. Low Temp. Phys. B* **7**, 373 (1978).
5. M. Rasolt, T. Edis, and Z. Tesanovic, *Phys. Rev. Lett.* **66**, 292 (1991).
6. P. Minnhagen and P. Olsson, *Phys. Rev. B* **45**, 5722 (1992).
7. A.T. Fiory, A.F. Hebard, P.M. Mankiewich *et al.*, *Phys. Rev. Lett.* **61**, 1419 (1988).
8. N.-C. Yeh and C. C. Tsuei, *Phys. Rev. B* **39**, 9708 (1989).
9. V.A. Gasparov, *Physica C* **178**, 449 (1991).
10. S. Vadlamannati, Q. Li, T. Venkatesan *et al.*, *Phys. Rev. B* **44**, 7094 (1991).
11. Y. Matsuda, S. Komiyama, T. Terashima *et al.*, *Phys. Rev. Lett.* **69**, 3228 (1992).
12. D. Norton and D. Lowndes, *Phys. Rev. B* **48**, 6460 (1993).
13. S. Martin, A.T. Fiory, R. M. Fleming *et al.*, *Phys. Rev. Lett.*, **62**, 677 (1989).
14. S.N. Artemenko, I.G. Gorlova and Yu.I. Latishev, *Phys. Lett. A* **138**, 428 (1989).
15. D.H. Kim, A.M. Goldman, J.H. Kang *et al.*, *Phys. Rev. B* **40**, 8834 (1989).
16. L.C. Davis, M.R. Beasley, and D.J. Scalapino, *Phys. Rev. B* **42**, 99 (1990).
17. C.T. Rogers and K.E. Myers J. N. Eckstein *et al.*, *Phys. Rev. Lett.* **69**, 160 (1992).
18. J.M. Repaci, C. Kwon, Qi Li *et al.*, *Phys. Rev. B* **54**, 9674 (1996).
19. M.R. Beasley, J.E. Mooij, and T.P. Orlando, *Phys. Rev. Lett.* **42**, 1165 (1979).
20. P. Minnhagen, B.I. Halperin, D.R. Nelson *et al.*, *Phys. Rev. B* **23**, 5745 (1981); *Rev. Mod. Phys.* **59**, 1001 (1987).
21. V. Ambegaokar, B.I. Halperin, D.R. Nelson *et al.*, *Phys. Rev. Lett.* **40**, 783 (1978); *Phys. Rev. B* **21**, 1806 (1980).
22. B.J. Halperin and D.R. Nelson, *J. Low Temp. Phys.* **36**, 599 (1979).
23. J. Bardeen and M.J. Stephen, *Phys. Rev.* **140**, A1197 (1965).
24. V.A. Gasparov, I. Batov, Qi Li, *et al.*, *Physica B* **284-288**, 1021 (2000); *Czechoslovak J. Phys.* **46** (Suppl. S3)1401 (1996); *Proc. SPIE* **2697**, 391 (1996); *Phys.of Low-Dim. Str.* **6**, n.12, 36 (1995).
25. Qi Li, X.X. Xi, X.D. Wu *et al.*, *Phys. Rev. Lett.* **64**, 3086 (1990).
26. C. Kwon, Qi Li, I. Takeuchi *et al.*, *Physica C* **266**, 75 (1996).
27. D. Chrisey and J. Horwitz, *Pulsed Laser Deposition, Present and Future*, Wiley, (1994).
28. V.A. Gasparov and A.P. Oganesyan, *Physica C* **178**, 445 (1991).
29. A. Gauzzi, J. Le Cochec, G. Lamura *et al.*, *Rev. Sci. Instr.* **71**, 2147 (2000).
30. A.T. Fiory, A.F. Hebard, P.M. Mankievich *et al.*, *Appl. Phys. Lett.* **52**, 2165 (1988).

31. B. Jeanneret, J.L. Gavilano, G.A. Racine *et al.*, *Appl. Phys. Lett.* **55**, 2336 (1989).
32. V.A. Gasparov, N.S. Sidorov, I.I. Zverkova, *et al.*, *JETP* (to be published).
33. L. Lyard, P. Samuely, P. Szabo *et al.*, *Phys. Rev. B* **66**, 180502(R) (2002).
34. M. Tinkham, *Introduction to Superconductivity* (McGraw Hill, New York, 1996), 2nd ed., p. 381.
35. L. Drabeck, K. Holczer, and G. Gruner *et al.*, *Phys. Rev. B* **42**, 10020 (1990)
36. E.H. Brandt, *Phys. Rev. Lett.* **68**, 3769 (1992).
37. D.S. Fisher, *Phys. Rev. B* **22**, 1190 (1980).
38. O. Brunner, L. Antognazza, J.-M. Triscone *et al.*, *Phys. Rev. Lett.* **67**, 1354 (1991).
39. C. Kwon, Qi Li, K.-C. Kim, *et al.*, *Superlattices and Microstructures*, **19**, 169 (1996).
40. A.F. Hebard and A.T. Fiory, *Phys. Rev. Lett.* **44**, 291 (1980).
41. K. Epstein, A.M. Goldman, and A.M. Kadin, *Phys. Rev. Lett.* **47**, 534 (1981).
42. K.H. Fischer, *Physica C* **193**, 401 (1992).
43. J.H.P.M. Emmen, V.A.M. Brabers and W.J.M. de Jonge, *Physica C* **176**, 137 (1991).
44. G. Blatter, M.V. Feigel'man, V.B. Geshkenbein, *et al.*, *Rev. Mod. Phys.*, **66**, 1125 (1994).
45. A.T. Fiory, A.F. Hebard, P.M. Mankiewich *et al.*, *Appl. Phys. Lett.* **52**, 2165 (1988).
46. J.R. Clem and M.W. Coffey, *Phys. Rev. B* **46**, 14662 (1992).
47. M.W. Coffey and J.R. Clem, *Phys. Rev. Lett.* **67**, 386 (1991).
48. C. J. van der Beek, M. Konczykowski, A. Abal'oshev *et al.*, *Phys. Rev. B* **66**, 024523 (2002).
49. Ch. Leemann, Ph. Flückiger, V. Marsico *et al.*, *Phys. Rev. Lett.*, **64**, 3082 (1990).